Aromatase Acetylation Patterns and Altered Activity in Response to Sirtuin Inhibition

Deborah Molehin[1], Isabel Castro-Piedras[1], Monica Sharma[1], Souad R. Sennoune[2], Daphne Arena[1], Pulak R. Manna[1], Kevin Pruitt[1],*

[1]Immunology and Molecular Microbiology, Texas Tech University Health Sciences Center, Lubbock, TX, USA

[2]Cell Physiology and Molecular Biophysics, Texas Tech University Health Sciences Center, Lubbock, TX, USA

Abstract

Aromatase, a cytochrome P450 member, is a key enzyme involved in estrogen biosynthesis and is dysregulated in the majority of breast cancers. Studies have shown that lysine deacetylase inhibitors (KDI) decrease aromatase expression in cancer cells, yet many unknowns remain regarding the mechanism by which this occurs. While advances have been made to clarify factors involved in the transcriptional regulation of the aromatase gene (CYP19A1). Yet, despite aromatase being a primary target for breast cancer therapy, its post-translational regulation has been virtually unexplored. Acetylation is a post-translational modification (PTM) known to alter the activity and stability of many oncoproteins and given the role of KDIs in regulating aromatase expression, we postulate that aromatase acetylation acts as a novel post-translational regulatory mechanism that impacts aromatase expression and/or activity in breast cancer. Liquid chromatography-tandem mass spectrometry (LC-MS/MS) analysis revealed that aromatase is basally acetylated on several lysine residues (108, 242, 262, 334, 352 and 354) in MCF-7 cells, and treatment with a SIRT-1 inhibitor induced additional acetylation (376, 390, 440 and 448). These acetylated lysine residues are in regions critical for aromatase activity. Site-directed mutagenesis and overexpression studies demonstrated that K108R/Q or K440R/Q mutations significantly altered aromatase activity in breast cancer cells without altering its subcellular localization.

Keywords

Aromatase; CYP19A1; KDAC; SIRT1; lysine deacetylase inhibitors

*Address correspondence to: Kevin Pruitt, Ph.D., Department of Immunology & Molecular Microbiology, Texas Tech University Health Sciences Center, 3601 4th Street, Lubbock, Texas 79430-6591, (ph) 806-743-2523; (fax) 806-743-2334, kevin.pruitt@ttuhsc.edu.

Introduction

Breast cancer in women represents 15% of all new cancer cases in the United States. Although a decline in death rates has been observed amongst women with breast cancer in the United States, reports from a Surveillance, Epidemiology and End Results programs (SEER) database predicts that approximately 266,120 will be diagnosed with breast cancer and 40,920 deaths will occur in 2018 (1). Estrogen receptor dependent breast cancers (ER+) constitute about 70% of breast cancer cases and patients are administered anti-hormonal therapies such as selective estrogen receptor modulators (SERM) or aromatase inhibitors (AIs) (2), with the aim of inhibiting intra-tumoral estrogen biosynthesis which drives tumor progression (3, 4).

Aromatase belongs to the cytochrome P450 superfamily, and is involved in steroidogenesis. While it is critical in human development and a wide range of physiological processes (5, 6), high expression of aromatase has been reported in tumors relative to non-neoplastic cells (5, 7–9) and linked with metastatic ER-dependent breast tumor cells (10, 11). Aromatase is an important therapeutic target in the treatment of post-menopausal breast cancer (12) and endometriosis (13). Aromatase overexpression in majority of breast cancers leads to chronic intra-tumoral increases in estrogens, which can impact the tumor microenvironment (14, 15). Interestingly, post-menopausal women with the highest quintile of plasma 17-β-estradiol (E_2) present with a significantly higher rate of breast cancer (BC) within 10 years compared with the lowest quintile (16, 17). Emerging data demonstrate that estrogen's impact extends well beyond ERα-mediated signaling (18) and engages both ERα-dependent and ERα-independent signaling (17–22). However, even though the relative contribution of estrogens to breast cancer exerting their impact via ERα, ERβ, or uncharacterized estrogen receptors (GPER-1/GPR30) remains unclear, it is clear that aromatase plays a critical role in the generation of the estrogen regardless of the specific signaling pathway that is activated downstream (18, 23, 24).

Post-translational modifications impacts the stability, localization and functionality of many proteins in cells including cancer cells (25, 26). With respect to aromatase protein, little is known about how aromatase is modified post-translationally and the possible implications of these modifications. Recent studies have shown that deacetylase inhibition sensitizes AI-resistant tumors overexpressing aromatase (27, 28). However, post-translational regulation of aromatase was not investigated in these studies. Also recently, a phase I clinical trial of panobinostat in combination with letrozole in postmenopausal women, proved efficacious in the treatment of metastatic breast cancer (29). Based on recent reports of the effect of lysine deacetylases (KDACs) on aromatase enzyme in breast cancer (30, 31), this present study aims to understand the mechanism by which the KDAC, Sirtuin-1 (SIRT-1), post-translationally regulate aromatase proteins and to evaluate the functional implications of acetylation marks on aromatase activity and estrogen biosynthesis.

Materials and methods

Cell culture

Cell lines were obtained from the American Type Culture Collection (ATCC, Manassas, VA, USA). MDA-MB 231 (HTB-26), JEG-3 (HTB-36) and HEK293 (CRL-1573) were cultured in D-MEM while T47D cells (HTB-133) and MCF-7 cells (HTB-22) were cultured in RPMI-1640 and MEM supplemented with 0.07–0.1% insulin respectively (Sigma-Aldrich; St. Louis, MO, USA). All culture media were supplemented with 10% fetal bovine serum and 1% penicillin/streptomycin (Invitrogen; Carlsbad, CA, USA). Cell lines were obtained between 2014 and 2017, immediately frozen down in liquid nitrogen, hence cells were cultured for less than 6 months. For enzyme inhibition studies, cells were treated with dimethyl sulfoxide (DMSO) vehicle control or varying concentrations of SIRT-1 inhibitor IV (566325; Millipore; Burlington, MA, USA) as noted in the figure legends.

Endpoint Polymerase Chain Reaction

Total RNA was isolated from cells using Pure-link RNA mini kit (Invitrogen), and 2μg of RNA reverse transcribed with Moloney murine leukemia virus Reverse Transcriptase (Promega; Madison, WI, USA). Intron-spanning primers were designed for each specific target DNA and gene expression measured by endpoint PCR using JumpStart RedTaq (Sigma). Human aromatase forward and reverse primers used were 5'-GGCAGTGCCTGCAACTACTA-3', 5'-GTCACCTCCTCCAACCTGTC-3' and β-actin were 5'-GGACTTCGAGCAAGAGATGG-3', 5'-AGCACTGTGTTGGCGTACAG-3'. Veriti 96-well thermal cycler (Applied Biosystems; Foster City, CA, USA) and Gel DOC EZ imager (Bio-Rad; Hercules, CA, USA) were used for PCR analyses.

Western blots

Protein samples were extracted from cells. Antibodies used include: aromatase (ab124776; Abcam; Cambridge, United Kingdom), V5-tag (ab27671; Abcam), Calnexin (ab22595; Abcam), Gapdh and β-actin (SC-47724 and −47778; Santa Cruz Biotechnology; Dallas, TX, USA). Proteins transferred onto polyvinylidene fluoride (PVDF) membranes (Millipore) were blotted with specific primary antibodies and horseradish peroxidase-conjugated secondary antibodies. Immunoblots were visualized by enhanced chemiluminescence on premium X-ray films (Phenix Research; Candler, NC, USA). Densitometric analyses of images were performed using Image Processing and Analysis in Java (ImageJ) software from three independent experiments.

Enzyme-linked Immunosorbent Assay

Cells seeded in charcoal stripped serum (CSS; Thermofisher; Waltham, MA, USA) media for 24 hours, were treated with DMSO or different doses of inhibitor IV for 4 hours, starting with half its IC50 value (63nM determined against SIRT-1 enzymes purified from mammalian cell) (32). Cells were supplemented with/without 10nM Androstenedione (Sigma-Aldrich). Supernatant culture media was evaluated for estrogen production using estradiol ELISA Kit (Cayman Chemical; Ann Arbor, MI, USA) following manufacturer's protocol at 412nm absorbance using an Infinite M100 PRO Quadruple monochromator

microplate reader (Tecan; Mannedorf, Switzerland). Standard curve and estradiol concentrations determined with Cayman ELISA competitive analysis tool.

Immunoprecipitation

Cells were seeded and harvested after 48 hours in either acetylation lysis buffer (acKIP) (1% Triton X-100, 0.5% NP-40, 150mM NaCl, 50mM Tris (pH 7.4), 10% glycerol, with complete protease inhibitors (Invitrogen), 1μM Trichostatin A (TSA) and 1mM nicotinamide) for acetylation studies, or in Radio-immunoprecipitation assay (RIPA) lysis buffer (pH 8.0) with protease inhibitors for ubiquitination, sumoylation and methylation analysis. Protein concentration quantified by BCA method (Thermofisher) and 2mg protein subjected to immunoprecipitation using either 1.5μg of normal mouse/rabbit IgG (control) or acetyl-lysine antibody (05–515, Millipore) or anti-aromatase antibody (ab124476; Abcam), anti-Sumo-1 (ab11672; Abcam), anti-pan methyl lysine (ab7315; Abcam), anti-dimethyl lysine (ab23366; Abcam) and anti-ubiquitin (STI200; Millipore). Protein-antibody-complexes were incubated with precleared Protein-G dynabeads (Invitrogen) on variable speed nutator (Fisher). Immune complexes were subjected to heat by boiling for 15 minutes, and analyzed by polyacrylamide gel electrophoresis using 4–12% bolt gel systems (Invitrogen).

Liquid chromatography/electrospray tandem mass spectrometry (LC-MS/MS).

MCF-7 cells were seeded and incubated at 37°C with either 20% or 2.5% O_2. Cells were treated when they reached 70–80% confluence with either DMSO or 32nM inhibitor IV for 10mins. Cells were lysed with acKIP buffer and protein extracts incubated with 4μg anti-aromatase antibody (ab124776; Abcam) overnight. Protein-G dynabeads were added to the antibody-protein-complex and incubated for 2 hours. Immunoprecipitates were shipped to Applied Biomics Inc. (Hayward, CA, USA) for acetylation site identification by LC-MS/MS mass spectrometry.

V5-Aromatase pcDNA3.1+ construct generation

The full length Cyp19A1 gene was obtained by a phusion high fidelity polymerase (New England Biolabs (NEB); Ipswich, MA) PCR. The template plasmid PLX304-V5-Arom was purchased from Harvard plasmid depository (HsCD00418838). Synthetic nucleotide primers (Supplementary Table 1) used were designed with V5-epitope tag either at the amino (-NH_2) or carboxyl (-COOH) terminus. The 1.5kb DNA product was subcloned into NheI/Not1 restriction enzyme sites of pcDNA3.1+ mammalian expression plasmid (Thermofisher) using T4 DNA ligase (Invitrogen). MAX efficiency competent cells (Sbtl2; Thermofisher) were transformed with ligation mixture, and plated on LB-ampicillin agar at 37°C overnight. Bacteria colonies were screened and plasmids extracted by QIAprep spin miniprep kit (Qiagen; Hilden, Germany). Plasmids isolated were subjected to NheI and NotI restriction digest, and fragments resolved on 1% agarose gel (Bio-Rad) in 1X TAE buffer. Sanger plasmid sequencing was used to confirm the DNA sequences.

Small interfering RNA (siRNA)-mediated knockdown and expression plasmid transfections

MCF-7 cells were seeded 24 hours prior to transfection with 50nM of non-target control siRNA (D-001210-01-05; Dharmacon, Lafayette, CO, USA) or SIRT-1 siGenome smartpool siRNA (M-003540-01-0010; Dharmacon) (Supplementary Table 2), using RNAi MAX lipofectamine reagent (Thermofisher) for 48hrs to study the effect of SIRT-1 downregulation. To investigate the effect of aromatase overexpression, cells were transfected with 1ug/well empty vector or with N-V5 or C-V5 tagged aromatase plasmid using Lipofectamine P3000 reagent and opti-MEM reduced serum media (Thermofisher) at 37°C following manufacturer's instructions. Protein or total RNA samples were extracted after 48 hours of transfection (HEK293) or 24 hours from other cells. Stable transfectants were selected with 900ug/ml Neomycin G418 (Sigma) for HEK293 cells and 600ug/ml for MCF-7 cells.

Site directed mutagenesis

pcDNA3.1-V5-Aromatase plasmids were subjected to site directed mutagenesis with nucleotide primers (Supplementary Table 3) designed using the quikchange mutagenesis primer design tool and kit (Agilent technologies; Santa Clara, CA, USA) following manufacturer protocol. Plasmids were transformed into XL10 Gold ultra-competent cells, and plated on ampicillin impregnated LB-agar overnight at 37°C. Bacteria colonies were screened and plasmids purified using miniprep kit. Sanger plasmid sequencing was done to validate the mutations.

Immunofluorescence

Cells were seeded onto coverslips (12mm) in a 60mm tissue culture dish. The cells were washed with PBS and fixed with 4% paraformaldehyde, quenched with 50mM ammonium chloride (NH_4Cl) in PBS. Non-specific binding was blocked with 5% Bovine serum albumin (BSA) in PBS (blocking buffer), followed by a 1 hour incubation of anti V5-epitope tag (Abcam: ab27671; 1/5000) and anti calnexin (Abcam; ab22595; 1/250) antibody. Anti-rabbit secondary antibodies Alexa fluor (#568; 1/300: phalloidin 488; 1/300: Thermofisher) or anti-mouse secondary antibody Alexa fluor 647 (1/5000) for 1 hour in the dark at room temperature. The samples were mounted with prolong gold antifade mounting solution with DAPI (Thermofisher). Images were captured using a Nikon T-1E laser scanning confocal microscopy, with a 60x objective, and analyzed with NIS software.

Endoplasmic reticulum fractionation

Stably transfected HEK293 cells were plated and allowed to reach 80% confluence. Cells were trypsinized, washed with 1X PBS and pelleted at 600x g for 5 mins. Fractionation was carried out using endoplasmic reticulum Isolation Kit (ER0100; Sigma-Aldrich) following manufacturer protocol. Protein fractions were quantified and analyzed by western blots.

In silico analysis

Aromatase protein sequence was obtained from National Center for Biotechnology Information (NCBI; NP_112503.1). Multiple sequence alignment of aromatase protein across different organisms was performed using Clustal Omega software (http://

www.ebi.ac.uk/Tools/msa/clustalo/). The structure and acetylated lysine residues on aromatase were modeled using the Protein Homology analogY Recognition Engine version 2 (Phyre2; http://www.sbg.bio.ic.ac.uk/phyre2), and the PredictProtein software (https://www.predictprotein.org/). ModPred tool was used to predict and analyze concurrently several PTM modifications on aromatase protein (33).

Statistical analysis

Unpaired student's t-tests and two-way analysis of variance (ANOVA) were performed using GraphPad Prism software, to assess whether differences observed in the various experiments were significant. All results are expressed as mean ± SEM and considered significant at $p<0.05$.

Results:

Aromatase is expressed in multiple cancer cell lines and enzymatic activity is regulated by SIRT-1 inhibition.

In order to assess the short-term impact of lysine deacetylase inhibitor (KDI)-mediated regulation of aromatase, we first established the basal expression of aromatase across three cancer cell lines. JEG3 cells were included in this study because of their high expression of aromatase protein. Reverse transcriptase polymerase chain reaction (RT-PCR) analysis using intron-spanning primers and Western blot analysis using aromatase-specific antibodies revealed expression of aromatase in all three cell lines examined (Supplementary Fig. S1A, B). Previous studies revealed that decreased aromatase protein levels had direct bearing on aromatase activity when cells were treated with SIRT-1 inhibitor for 24hrs. We decided to investigate whether a SIRT-1 inhibitor had a direct effect on aromatase activity by treating the cells for a shorter duration. The effect of a preclinical SIRT-1-specific KDI (inhibitor IV) on aromatase activity in MCF-7 breast cancer cell line showed a statistically significant dose-dependent reduction in 17-β estradiol (E2) levels, without a decrease in aromatase protein levels, 4 hours post KDI administration (Fig. 1a). Small interfering RNA (siRNA) mediated SIRT-1 knockdown resulted in a 65% and 45% downregulation of SIRT-1 and aromatase protein levels, respectively. SIRT-1 downregulation led to a statistically significant decrease (p=0.02) in estradiol levels in MCF-7 cells (Fig. 1b).

Aromatase protein is basally acetylated and KDI further induces acetylation in breast cancer and placental choriocarcinoma cell lines.

To investigate the role of aromatase acetylation in different cancer context, we decided to include MDA-MB 231 and JEG3 cell lines in the analysis. Immunoprecipitation and Western blot analyses using acetyl-lysine specific monoclonal antibodies showed that aromatase is acetylated in all cancer cell lines tested (Fig. 2a). The lowest basal acetylation signal was observed in MCF-7 cells when compared to the other two cell lines (Fig. 2b). Time-dependent effect of inhibitor IV on aromatase protein in MCF-7cell lines showed that induced acetylation signal peaked at 10 minutes post treatment and started to diminish over time (Fig. 2c). We observed a significant induction of aromatase acetylation in MCF-7 (p=0.02), but variable induction in MDA-MB-231 and JEG3 cells when compared to the untreated cell lines (Fig. 2d, and e).

Aromatase is acetylated at key lysine residues upon treatment with Inhibitor IV at atmospheric and physiological O$_2$.

To further probe aromatase acetylation induced by KDI in MCF-7 breast cancer cells, protein extracts were subjected to proteolytic analysis by LC-tandem mass spectrometry to identify acetylated lysine residues on aromatase protein. Results from LC-MS/MS were consistent with immunoprecipitation results which showed that aromatase is basally acetylated and further induced by inhibitor IV (Supplementary Fig. S2 and Supplementary Table S4). A total of 11 lysine residues were acetylated and according to structural and mutational studies (34) located in the β-sheets, helical and loop region connecting the transmembrane region of the protein (Table 1). We further subjected the cells to physiological oxygen conditions (2.5% O$_2$) in which the inhibitors are likely to be eliciting their effects *in vivo* to determine the effect of reduced oxygen tension on acetylation of aromatase. Notably, at physiological oxygen, we observed acetylation of a different lysine residue (Lys 440) in comparison to those from the atmospheric oxygen incubation conditions.

Solvent accessibility prediction of acetylated aromatase residues with PredictProtein software (35) revealed that majority of the residues are buried (55%), exposed (18%) or intermediate (27%) suggesting that most of the acetylated residues may be located on the luminal side of the endoplasmic reticulum. Since lysine acetylation neutralizes the positive charge on unmodified lysine, this post-translational modification on aromatase could be playing a significant role in the regulation of properties of the domains in which it occurs.

Homology search revealed a total of 6 conserved lysine residues of the 11 acetylated residues amongst P450 aromatase of different organisms analyzed, however we only show the sequence alignment data for K108 and K440, since these lysines were further analyzed in this study (Fig. 3a). The proximity of the acetylated lysine residues to the enzyme catalytic site and substrate binding region (pocket region) was analyzed based on the crystal structure of human *CYP19A1* (RCSB PDB ID: 3S7S). Results showed that of all the conserved lysine residues, only Lys 440 had a +3 amino acids (aa) closeness to the catalytic site, which is fundamental in the conversion of androgen substrate to estrogen by aromatase enzyme whereas Lys 108, 354, 390, 440 and 448 had a proximity of +/− 10 aa to the substrate binding region critical to the accessibility of the androgen substrate. Overall, we observed a repeated occurrence in the acetylation of Lys 108 which has been shown by other studies to be involved in the association of aromatase and cytochrome P450.

Aromatase overexpression increased estradiol levels with androgen substrate in transiently transfected MCF-7 cells:

To determine the effect of aromatase overexpression on estradiol levels, aromatase gene was cloned into pcDNA3.1 (+) vector with V5-tag either at the N- or C-terminus. MCF-7 cells transfected with N-V5-aromatase plasmids over a course of time showed peak V5-tag expression at 24hrs (Fig. 3b); however, the highest V5-tag expression was observed at 48hrs in HEK293 cells (Supplementary Fig. S1C). Therefore, further transfection experiments were done at those times for the different cell lines. Estradiol quantification in MCF-7 cells transfected with aromatase constructs showed minimal difference between empty vector and

V5-aromatase transfected cells (Supplementary Fig. S1D). Upon treatment with 10nM androstenedione (A4) substrate, there was a marked difference in estradiol levels (at least >100 fold) between the empty vector and V5-aromatase transfected cells (both N-and C-V5 tagged aromatase) with a significant difference observed after 2 days incubation (Supplementary Fig. S1E).

K108 and K440 mutations altered aromatase activity in breast cancer cell lines:

Acetylation has been shown by many studies to affect the function of an enzyme. We wanted to determine if the ability of aromatase to convert androgen to estrogen is regulated by specific lysines that are acetylated. Lysine 108 is conserved across species, and according to structural analysis, is located in the substrate binding region. We decided to determine its role in regulating cancer cell production of estrogens using lysine point mutants. Because K440 has a proximity of 3 aa to the heme binding region we reasoned that any alteration of this residue might influence aromatase activity. In order to test the role of these lysines, we generated K108R/K440R and K108Q/K440Q aromatase point mutants and transfected MCF-7, T47D, and MDA-MB 231 cells with either of the plasmids. As a substitute, arginine (R) and glutamine (Q) were chosen because lysine acetylation neutralizes the positive charge, and although, these residues are similar in length to lysine, R maintains its charge while Q is neutral. Overexpression of N-V5-Aromatase constructs was confirmed by expression of mRNA (Fig. 3c, 4b, and 5b), and protein (Fig. 3d, 4c, and 5c) for WT and all four point mutants in MCF-7, T47D and MDA-MB231 cells.

In MCF-7 cells, there was no change in E2 levels with the expression of K108R when compared with the WT, however there was a significant increase (p=0.0172) in E2 levels with K108Q mutant (Fig. 3e). On the other hand, a significant decrease (p=0.0159) in E2 levels was observed with K440R mutant and an increase (p=0.0124) with K440Q mutants when matched with the WT (Fig. 3f). In T47D cells, another ER positive cell line, K108R mutant caused a significant increase (p<0.0001) in E2 levels whereas K108Q significantly reduced (p=0.0182) E2 levels relative to the WT (Fig. 4d). Similarly, a significant increase (p<0.0001) in E2 levels was observed with K440R mutant while a decrease (p=0.0004) was seen with K440Q mutants when matched to the WT (Fig. 4e). In triple negative breast cancer MDA-MB-231 cells, we observed a significant increase (p<0.0001) in E2 levels with K108R mutant and a decrease (p=0.0122) with K108Q relative to the WT (Fig. 5d). A similar trend was observed with K440R mutant (p=0.0117) but no difference in E2 was observed with K440Q when compared to the WT (Fig. 5e).

K108/K440 mutations does not change subcellular localization of aromatase protein:

Acetylation has been reported to change subcellular location of some proteins. Here, immunofluorescence staining detected N-V5-aromatase WT, K108R, K108Q, K440R, and K440Q in the endoplasmic reticulum of stably transfected HEK293 cells (Fig. 6a). Endoplasmic reticulum fractionation also confirmed the protein expression of N-V5-aromatase constructs (Fig. 6b). Colocalization studies revealed an overlap of the overexpressed aromatase N-V5-aromatase WT and mutant proteins with calnexin, an endoplasmic reticulum marker protein in stably transfected HEK293 cells (Supplementary Fig. S3). This demonstrates that these point mutants localize to the endoplasmic reticulum

and these specific mutations do not cause a relocation of the protein to another subcellular compartment in these cells.

Aromatase protein might be regulated by other post-translational modifications.

We predicted that with acetylation mimetics, aromatase activity would decrease, and with deacetylation mimetics, E2 levels would either increase or remain unchanged. We observed a contrary trend in MCF-7 cells and this prompted us to probe other possible lysine PTMs that might be working in concert with acetylation to regulate aromatase. *In silico* analysis using ModPred tool revealed that other lysine PTMs might be involved in the regulation of aromatase protein expression at K108 and K440 locations (Table 2). In addition, immunoprecipitation and Western blot analyses show for the first time that aromatase protein is basally sumoylated, methylated and possibly ubiquitinated in MCF-7 cells (Fig. 7a). Next, we decided to investigate whether any of this PTMs played a role in the phenotype observed when K108Q, K440R, or K440Q were transfected into MCF-7 cells. We subjected stably transfected MCF-7 cells to immunoprecipitation using antibodies specific to sumoylated, methylated and ubiquitinated proteins. Interestingly, results show evidence of that the N-V5-Aromatase WT and mutant proteins were ubiquitinated (Fig. 7b), sumoylated (Fig. 7c), and methylated (Fig. 7d) in MCF-7 cells.

Discussion

Numerous biological systems depend on the proper balance of androgens and estrogens. Aromatase uniquely has the capacity to deplete androgen levels while simultaneously boosting estrogen reservoirs. This critical conversion is the foundation for diverse biological processes and because of the impact of hormonal imbalances on numerous cell types, it is perhaps not surprising that aromatase is frequently elevated in tumors and drives hormone-dependent breast and endometrial tumor progression. Because of its contribution to multiple facets of tumor progression, numerous efforts have led to the generation of aromatase inhibitors which are frequently used in the clinic. In fact, clinical trials demonstrated higher benefit in patients treated with aromatase inhibitors compared to tamoxifen (36) and recommendations have been made to incorporate an AI to reduce the risk of breast cancer recurrence (37). While AI therapy is effective against hormone-dependent cancers, the problem of resistance to endocrine therapy is the leading cause of cancer death. Despite the clear importance of aromatase in normal and pathophysiological settings, much remains unknown about how it is regulated. Our findings here provide additional insight into its post-translational regulation beyond phosphorylation. Our study was prompted by two earlier seminal observations. First, it was shown that treatment of MCF-7 cells for 24 hours with the clinical lysine deacetylase inhibitor, panobinostat, led to a reduction in aromatase mRNA (30). Panobinostat inhibits class I/II deacetylases, but not the class III sirtuin deacetylases. Second, we reported that inhibition of sirtuin-1/2 over the same time frame and longer, led to decreased aromatase mRNA and protein (31). Both of these studies focused on the impact of higher doses of KDAC inhibitors on the transcriptional regulation of *CYP19A1*, yet the short-term impact of these agents was not explored. Here we show that aromatase is also regulated by sirtuin deacetylases and its enzymatic activity altered when cells were treated with low doses of SIRT-1 inhibitor IV over a short time frame, which suggested that a post-

translational regulation of aromatase may account for this change and we reasoned that acetylation could be the key. Based on a series of acetyl-lysine immunoprecipitation, Western blotting and LC-MS/MS analyses we have demonstrated that aromatase undergoes protein acetylation as another regulatory mechanism.

This study provides the first report of aromatase acetylation as a novel post-translational modification and has generated the very first map of 11 acetylation sites that are either basally present or induced by a preclinical SIRT-1 inhibitor IV. Six of these lysines were found to be conserved across the analyzed organisms suggesting that these lysine residues play a crucial role in the aromatase function. Other lysine residues which did not appear conserved amongst homologues but specific to human aromatase might be implicative of adaptive plasticity in humans. K108 located in the substrate binding region, has been shown to be key in the interaction between aromatase and its obligatory binding partner NADPH cytochrome P450 reductase (38), which essentially transfers electrons to the heme group of aromatase, during estrogen biosynthesis from androgen substrate, in a process known as aromatization. We found K108 to be basally acetylated and deacetylation of K108 will erase the positive charge as will substitution of K with Q. Lysine 440 is situated 3 aa away from the catalytic site buried in the heme binding region of aromatase protein, where aromatization takes place (39).

Historically, histone or lysine deacetylases have been associated with formation of heterochromatin and the epigenetic repression of tumor suppressor genes (40). However, new evidence demonstrates that acetylation directly modulates the activity of non-histone oncoproteins (41, 42), and tumor suppressors (43, 44). With the recent approval of the first deacetylase inhibitors for cancer treatment (45), and their phase I testing for breast cancer (29), it is important to fully characterize additional mechanisms of tumor regression.

Herein, functional analysis of K108 and K440 residues showed a decrease in aromatase activity with K108Q and K440Q mutants when compared with WT in T47D and MDA-MB −231 breast cancer cells. Moreover, with K108R and K440R mutants, E2 levels either remained unchanged or increased as predicted in these cell lines. This suggest that these lysine residues are important in the function of aromatase to convert androgen to estrogen and that acetylation is a novel regulator of aromatase activity at these sites in these cells. Contrary to the observed trend in these cell lines, E2 levels increased with K108Q and K440Q mutants and decreased with K440R mutants in MCF-7 cells, this perhaps is indicative of other possible post translational modifications in a cell-type specific manner regulating aromatase activity. Immunoprecipitation analysis revealed that sumoylation, methylation, and possibly ubiquitination are another set of PTMs that might be regulating endogenous aromatase. Here, ectopically overexpressed aromatase WT, K108 and K440 mutants were sumoylated, methylated and to a lesser extent ubiquitinated. Cross-talk between PTMs are increasingly reported on many proteins to generate a PTM code, which can be read by specific effectors to positively/negatively regulate downstream processes. Perhaps, these modifications might be playing an inhibitory role in the case of K440R while positively regulating aromatase activity in K108Q and K440Q mutants in MCF-7 cells. Alternatively, if these specific lysines undergo methylation or sumoylation modifications, then changing it to Q or another residue could prevent this modification from taking place.

Arginine residues are capable of more electrostatic interactions when matched with lysine residues owing to the presence of the guanidinium group on arginine which allows for stronger ionic interactions, hydrogen bonds and salt bridge formations (46). One would imagine that substituting a positively charged residue with a neutral residue would have significant implications on the function of an enzyme. Also, the change in lysine residue to arginine at position 440 could subject K440R to methylation, which could have led to decreased aromatase protein expression and subsequently decreased activity. Additional studies are needed to provide insight into the dynamics and complexity of PTM crosstalk on aromatase in MCF-7 cells.

Here, we show that in T47D and MDA-MB-231 cells, K108Q and K440Q reduced ability of aromatase enzyme to convert androgens to estrogens. Mutational studies by Hong and colleagues (38) showed that K108Q decreased aromatase activity. Although they did not investigate the regulation of aromatase by acetylation, they observed a marked decline in aromatase activity with K108Q mutants in Chinese Hamster Ovary (CHO) cells, and concluded that the substrate binding to the enzyme was unhindered. However the binding of aromatase to its partner was altered, hence a reduced electron transfer and ultimately decreased enzymatic activity. In this study we did not assess the impact of this mutation on the interaction between aromatase and reductase. However, our results are consistent with the effect of K108Q mutation on aromatase activity as seen in Hong's study (38). Overall, we demonstrate that alteration of K108 and K440 residues decreased aromatase activity in T47D and 231 cells.

Recent studies demonstrated that combination therapies including KDIs are effective in sensitizing AI-resistant tumors and breast cancer cells (27, 47). Previously, we showed that inhibition of sirtuin deacetylases caused reduced aromatase protein (31). We now demonstrate that at significantly lower doses, SIRT-1 inhibition impacts aromatase acetylation which concomitantly influences estrogen biosynthesis by regulating aromatase activity. Finally, there is evidence that aromatase (48, 49) and SIRT-1 (50, 51) are regulated in an oxygen dependent manner and may provide meaning to the difference in some acetylation sites under physiological vs. atmospheric O_2 culture conditions. Overall, we now know that aromatase is regulated at yet another level and treatment with specific KDIs may impact both its transcription as well as its acetylation. Thus understanding the gaps in our knowledge regarding an important but poorly understood post-translational aromatase regulation could help identify novel therapeutic vulnerabilities.

Supplementary Material

Refer to Web version on PubMed Central for supplementary material.

Acknowledgement

Reference List

1. Noone AM, et al. (2017) Cancer Incidence and Survival Trends by Subtype Using Data from the Surveillance Epidemiology and End Results Program, 1992–2013. Cancer Epidemiol Biomarkers Prev 26(4):632–641. [PubMed: 27956436]

2. Piccolella M, et al. (2017) The small heat shock protein B8 (HSPB8) modulates proliferation and migration of breast cancer cells. Oncotarget 8(6):10400–10415. [PubMed: 28060751]

3. Santen RJ, et al. (2009) History of aromatase: saga of an important biological mediator and therapeutic target. Endocr Rev 30(4):343–375. [PubMed: 19389994]

4. Manna PR, Molehin D, & Ahmed AU (2016) Dysregulation of Aromatase in Breast, Endometrial, and Ovarian Cancers: An Overview of Therapeutic Strategies. Prog Mol Biol Transl Sci 144:487–537. [PubMed: 27865465]

5. Bulun SE (2014) Aromatase and estrogen receptor alpha deficiency. Fertil Steril 101(2):323–329. [PubMed: 24485503]

6. Blakemore J & Naftolin F (2016) Aromatase: Contributions to Physiology and Disease in Women and Men. Physiology (Bethesda) 31(4):258–269. [PubMed: 27252161]

7. Bulun SE, et al. (2012) Aromatase, breast cancer and obesity: a complex interaction. Trends Endocrinol Metab 23(2):83–89. [PubMed: 22169755]

8. Sasaki Y, et al. (2010) Immunolocalization of estrogen-producing and metabolizing enzymes in benign breast disease: comparison with normal breast and breast carcinoma. Cancer Sci 101(10):2286–2292. [PubMed: 20682005]

9. Shibuya R, et al. (2008) Intratumoral concentration of sex steroids and expression of sex steroid-producing enzymes in ductal carcinoma in situ of human breast. Endocr Relat Cancer 15(1):113–124. [PubMed: 18310280]

10. Mukhopadhyay KD, et al. (2015) Aromatase expression increases the survival and malignancy of estrogen receptor positive breast cancer cells. PLoS One 10(4):e0121136.

11. Zhou J, et al. (2001) Malignant breast epithelial cells stimulate aromatase expression via promoter II in human adipose fibroblasts: an epithelial-stromal interaction in breast tumors mediated by CCAAT/enhancer binding protein beta. Cancer Res 61(5):2328–2334. [PubMed: 11280806]

12. Johnston SR & Dowsett M (2003) Aromatase inhibitors for breast cancer: lessons from the laboratory. Nat Rev Cancer 3(11):821–831. [PubMed: 14668813]

13. Pavone ME & Bulun SE (2012) Aromatase inhibitors for the treatment of endometriosis. Fertil Steril 98(6):1370–1379. [PubMed: 22999792]

14. Chen S, et al. (2002) Transcriptional regulation of aromatase expression in human breast tissue. J Steroid Biochem Mol Biol 83(1–5):93–99. [PubMed: 12650705]

15. Zhao H, Zhou L, Shangguan AJ, & Bulun SE (2016) Aromatase expression and regulation in breast and endometrial cancer. J Mol Endocrinol 57(1):R19–33. [PubMed: 27067638]

16. Missmer SA, Eliassen AH, Barbieri RL, & Hankinson SE (2004) Endogenous estrogen, androgen, and progesterone concentrations and breast cancer risk among postmenopausal women. J Natl Cancer Inst 96(24):1856–1865. [PubMed: 15601642]

17. Kaaks R, et al. (2005) Postmenopausal serum androgens, oestrogens and breast cancer risk: the European prospective investigation into cancer and nutrition. Endocr Relat Cancer 12(4):1071–1082. [PubMed: 16322344]

18. Filardo EJ & Thomas P (2012) Minireview: G protein-coupled estrogen receptor-1, GPER-1: its mechanism of action and role in female reproductive cancer, renal and vascular physiology. Endocrinology 153(7):2953–2962. [PubMed: 22495674]

19. van Landeghem AA, Poortman J, Nabuurs M, & Thijssen JH (1985) Endogenous concentration and subcellular distribution of estrogens in normal and malignant human breast tissue. Cancer Res 45(6):2900–2906. [PubMed: 3986816]

20. Yager JD & Davidson NE (2006) Estrogen carcinogenesis in breast cancer. N Engl J Med 354(3):270–282. [PubMed: 16421368]

21. Catalano S, et al. (2009) Rapid estradiol/ERalpha signaling enhances aromatase enzymatic activity in breast cancer cells. Mol Endocrinol 23(10):1634–1645. [PubMed: 19556341]

22. Wang J, Gildea JJ, & Yue W (2013) Aromatase overexpression induces malignant changes in estrogen receptor alpha negative MCF-10A cells. Oncogene 32(44):5233–5240. [PubMed: 23178495]

23. Thomas C & Gustafsson JA (2011) The different roles of ER subtypes in cancer biology and therapy. Nat Rev Cancer 11(8):597–608. [PubMed: 21779010]

24. Mizukami Y (2010) In vivo functions of GPR30/GPER-1, a membrane receptor for estrogen: from discovery to functions in vivo. Endocr J 57(2):101–107. [PubMed: 19996532]

25. Drazic A, Myklebust LM, Ree R, & Arnesen T (2016) The world of protein acetylation. Biochim Biophys Acta 1864(10):1372–1401. [PubMed: 27296530]

26. Dushukyan N, et al. (2017) Phosphorylation and Ubiquitination Regulate Protein Phosphatase 5 Activity and Its Prosurvival Role in Kidney Cancer. Cell Rep 21(7):1883–1895. [PubMed: 29141220]

27. Kubo M, et al. (2013) Inhibition of the proliferation of acquired aromatase inhibitor-resistant breast cancer cells by histone deacetylase inhibitor LBH589 (panobinostat). Breast Cancer Res Treat 137(1):93–107. [PubMed: 23160924]

28. Sabnis GJ, et al. (2011) Functional activation of the estrogen receptor-alpha and aromatase by the HDAC inhibitor entinostat sensitizes ER-negative tumors to letrozole. Cancer Res 71(5):1893–1903. [PubMed: 21245100]

29. Tan WW, et al. (2016) Phase I Study of Panobinostat (LBH589) and Letrozole in Postmenopausal Metastatic Breast Cancer Patients. Clin Breast Cancer 16(2):82–86. [PubMed: 26774555]

30. Chen S, Ye J, Kijima I, & Evans D (2010) The HDAC inhibitor LBH589 (panobinostat) is an inhibitory modulator of aromatase gene expression. Proc Natl Acad Sci U S A 107(24):11032–11037. [PubMed: 20534486]

31. Holloway KR, et al. (2013) SIRT1 positively regulates breast cancer associated human aromatase (CYP19A1) expression. Mol Endocrinol 27(3):480–490. [PubMed: 23340254]

32. Napper AD, et al. (2005) Discovery of indoles as potent and selective inhibitors of the deacetylase SIRT1. J Med Chem 48(25):8045–8054. [PubMed: 16335928]

33. Pejaver V, et al. (2014) The structural and functional signatures of proteins that undergo multiple events of post-translational modification. Protein Sci 23(8):1077–1093. [PubMed: 24888500]

34. Chen S & Zhou D (1994) Functional domains of aromatase cytochrome P450 inferred from comparative analyses of amino acid sequences and substantiated by site-directed mutagenesis experiments. J Biol Chem 269(2):1564. [PubMed: 8288624]

35. Rost B, Yachdav G, & Liu J (2004) The PredictProtein server. Nucleic Acids Res 32(Web Server issue):W321–326. [PubMed: 15215403]

36. Bonneterre J, et al. (2001) Anastrozole is superior to tamoxifen as first-line therapy in hormone receptor positive advanced breast carcinoma. Cancer 92(9):2247–2258. [PubMed: 11745278]

37. Burstein HJ, et al. (2010) American Society of Clinical Oncology clinical practice guideline: update on adjuvant endocrine therapy for women with hormone receptor-positive breast cancer. J Clin Oncol 28(23):3784–3796. [PubMed: 20625130]

38. Hong Y, et al. (2009) Epitope characterization of an aromatase monoclonal antibody suitable for the assessment of intratumoral aromatase activity. PLoS One 4(11):e8050.

39. Ghosh D, Griswold J, Erman M, & Pangborn W (2010) X-ray structure of human aromatase reveals an androgen-specific active site. J Steroid Biochem Mol Biol 118(4–5):197–202. [PubMed: 19808095]

40. Pruitt K, et al. (2006) Inhibition of SIRT1 reactivates silenced cancer genes without loss of promoter DNA hypermethylation. PLoS Genet 2(3):e40.

41. Saxena M, et al. (2015) The sirtuins promote Dishevelled-1 scaffolding of TIAM1, Rac activation and cell migration. Oncogene 34(2):188–198. [PubMed: 24362520]

42. Pandey S, et al. (2015) A novel MeCP2 acetylation site regulates interaction with ATRX and HDAC1. Genes Cancer 6(9–10):408–421. [PubMed: 26622943]

43. Pearson M, et al. (2000) PML regulates p53 acetylation and premature senescence induced by oncogenic Ras. Nature 406(6792):207–210. [PubMed: 10910364]

44. Leduc C, et al. (2006) p14ARF promotes RB accumulation through inhibition of its Tip60-dependent acetylation. Oncogene 25(30):4147–4154. [PubMed: 16501607]

45. Mann BS, et al. (2007) FDA approval summary: vorinostat for treatment of advanced primary cutaneous T-cell lymphoma. Oncologist 12(10):1247–1252. [PubMed: 17962618]

46. Sokalingam S, Raghunathan G, Soundrarajan N, & Lee SG (2012) A study on the effect of surface lysine to arginine mutagenesis on protein stability and structure using green fluorescent protein. PLoS One 7(7):e40410.

47. Munster PN, et al. (2011) A phase II study of the histone deacetylase inhibitor vorinostat combined with tamoxifen for the treatment of patients with hormone therapy-resistant breast cancer. Br J Cancer 104(12):1828–1835. [PubMed: 21559012]

48. Yu RM, et al. (2015) Evidence for microRNA-mediated regulation of steroidogenesis by hypoxia. Environ Sci Technol 49(2):1138–1147. [PubMed: 25496461]

49. Kumar P & Mendelson CR (2011) Estrogen-related receptor gamma (ERRgamma) mediates oxygen-dependent induction of aromatase (CYP19) gene expression during human trophoblast differentiation. Mol Endocrinol 25(9):1513–1526. [PubMed: 21757507]

50. Lim JH, et al. (2010) Sirtuin 1 modulates cellular responses to hypoxia by deacetylating hypoxia-inducible factor 1alpha. Mol Cell 38(6):864–878. [PubMed: 20620956]

51. Chen R, et al. (2011) Hypoxia increases sirtuin 1 expression in a hypoxia-inducible factor-dependent manner. J Biol Chem 286(16):13869–13878. [PubMed: 21345792]

Implications:

These findings demonstrate a novel post-translational regulation of aromatase and uncover novel anti-cancer effects of deacetylase inhibitors; thus, providing new insight for ongoing development of deacetylase inhibitors as cancer therapeutics.
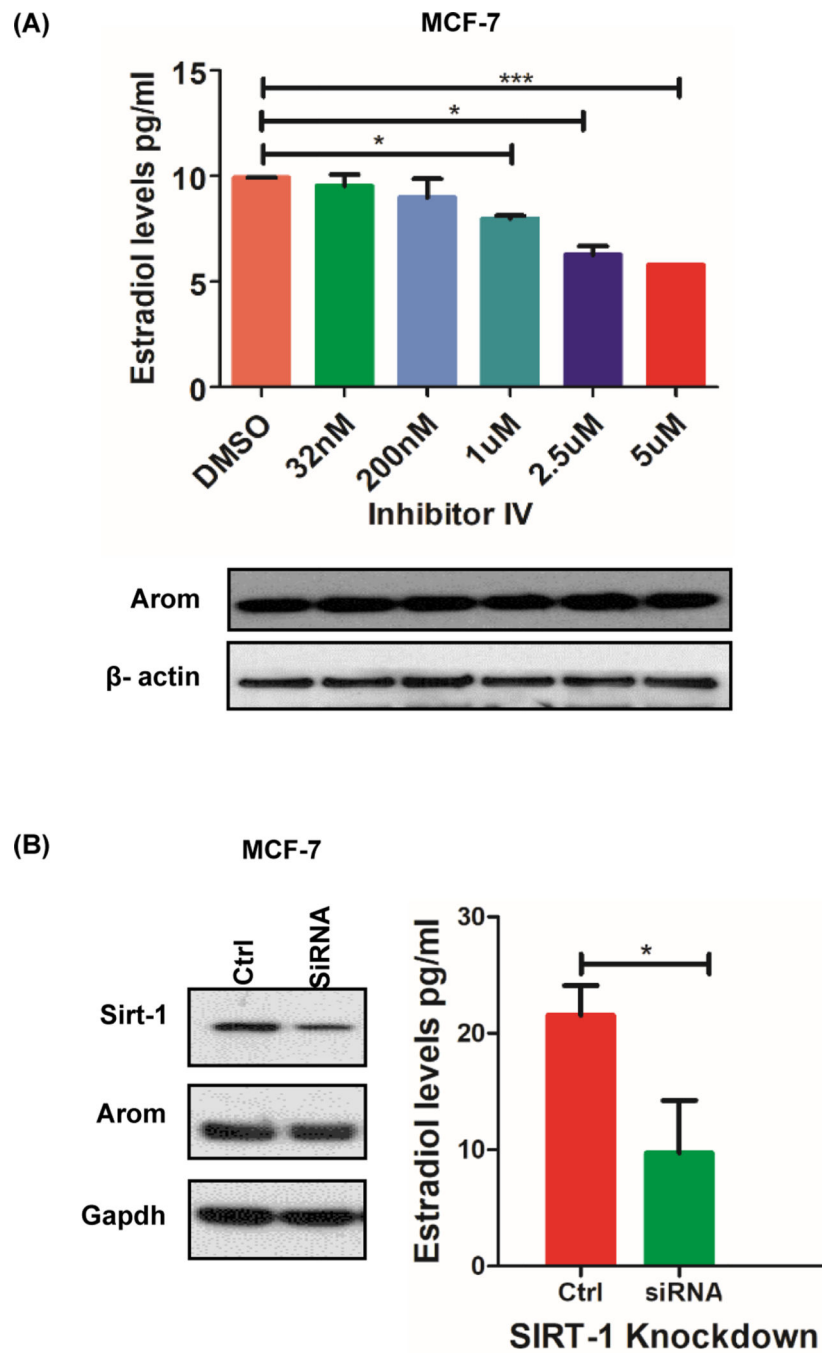
Figure 1: Sirtuin deacetylases regulate aromatase activity.
A, Aromatase activity and protein levels with increasing Sirtuin deacetylase inhibitor concentrations (32nM-5μM) when MCF-7 cells were treated for 4 hours. **B,** siRNA-mediated inhibition of SIRT-1 in MCF-7 cells decrease aromatase protein and activity when cells were treated for 48hrs. Data represented as mean ± SEM ***p =0.0008, * p<0.05 of three different experiments.
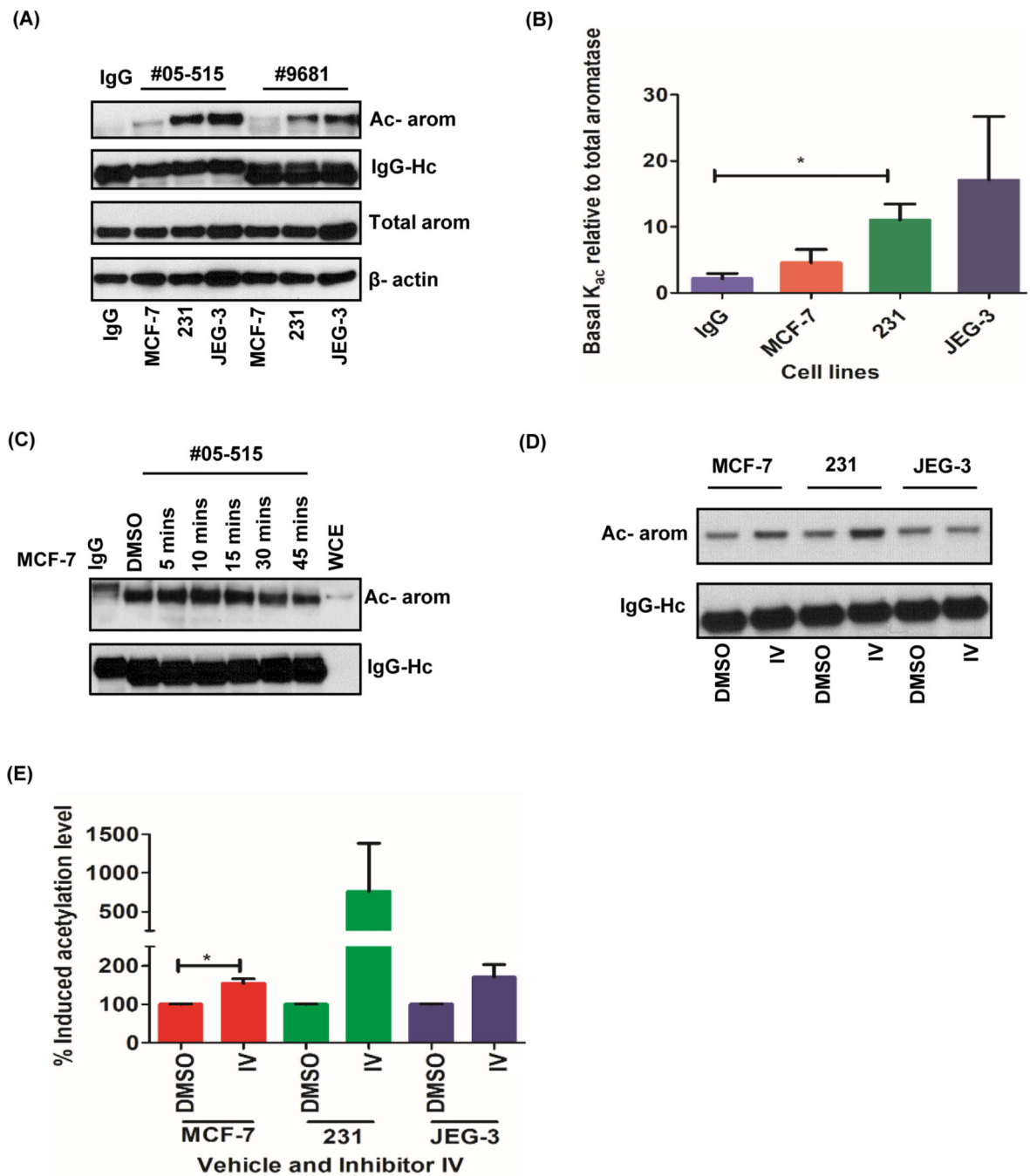
(A)

(B)

(C)

(D)

(E)

Figure 2: Aromatase protein is basally acetylated and induced by SIRT-1 inhibitor IV in cancer cells.

A, Basal aromatase protein acetylation pattern in MCF-7, MDA-MB 231 and JEG3 cells with acetyl-lysine antibody #05–515 and #9681. **B,** Densitometric analysis of the acetylated aromatase (Kac) relative to total aromatase images from #05–515 pull down assays. **C,** Time course of aromatase acetylation induced by inhibitor IV in MCF-7 cells. **D,** Induction of aromatase acetylation with 32nM inhibitor IV in MCF-7, MDA-MB 231 and JEG3 cells

when treated for 10 mins. **E,** Densitometric analysis of induced aromatase acetylation. Data represented as mean ± SEM* $p<0.05$ of three different experiments.

(A)


```
                 Substrate              Heme
                 108                    440

Bacteria    ----VRTWKERR   TTVQDARDYLRRV---
Fish        VHHVLKNGNYTS    PRACIG-KHMAMVMMK
Bird        VFHVMKHWNYVS    PRGCVG-KFIAMVMMK
Humans      MFHIMKHNHYSS    PRGCAG-KYIAMVMMK
Mouse       MFHVMKHSHYIS    PRGCAG-KYIAMVMMK
Rat         MVHVMKHSNYIS    PRSCAG-KYIAMVMMK
```

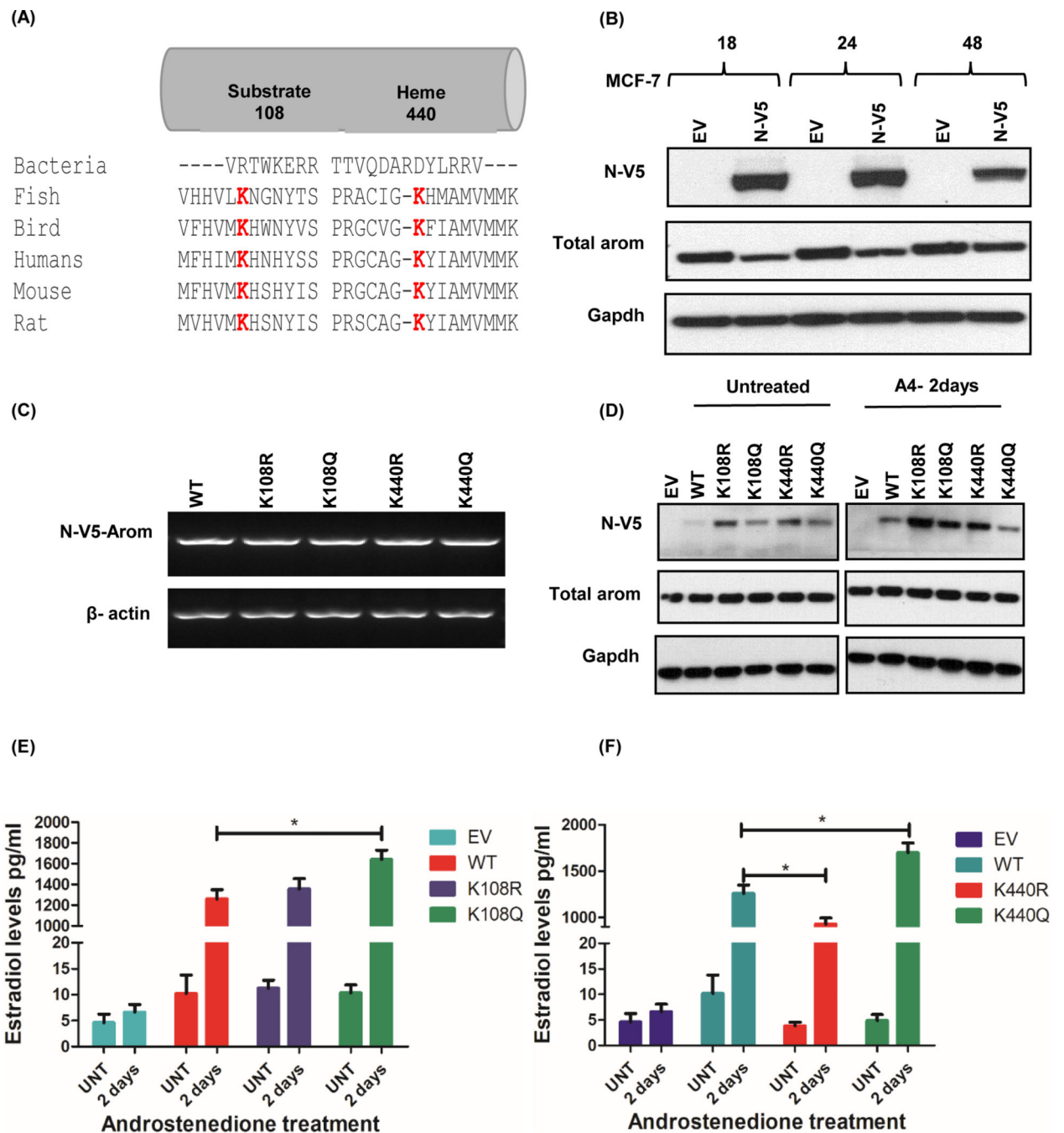**(B)**

(C)

(D)

(E)

(F)

Figure 3: Functional importance of conserved residues on aromatase activity by mutational studies in MCF-7 cells.

A, Multiple alignment of aromatase protein sequence across different organisms was performed using Clustal Omega software. The acetylated lysine residues (K) at positions 108 in the substrate binding region and 440 in the heme binding domain are conserved (red). **B,** Time course of N-V5-tagged aromatase-WT construct expression in MCF-7 cells. **C,** Transcript levels of V5-aromatase WT and mutant constructs and loading control beta actin in MCF-7 cells after 24hrs. **D,** Expression of N-terminally tagged V5-aromatase constructs,

endogenous aromatase (Total aromatase) and endogenous control Gapdh in MCF-7 cells untreated or treated with androstenedione for 2 days (A4–2days). **E,** Estradiol levels of V5-aromatase WT and K108R/K108Q transfected cells treated with/without 10nM androstenedione for 2 days (A4–2days). **F,** Estradiol levels of V5-aromatase WT and K440R/K440Q transfected cells with/without 10nM androstenedione after 2 days (A4–2 days). Data is representative of three independent experiments carried out in triplicates with mean ± SEM * $p<0.05$.
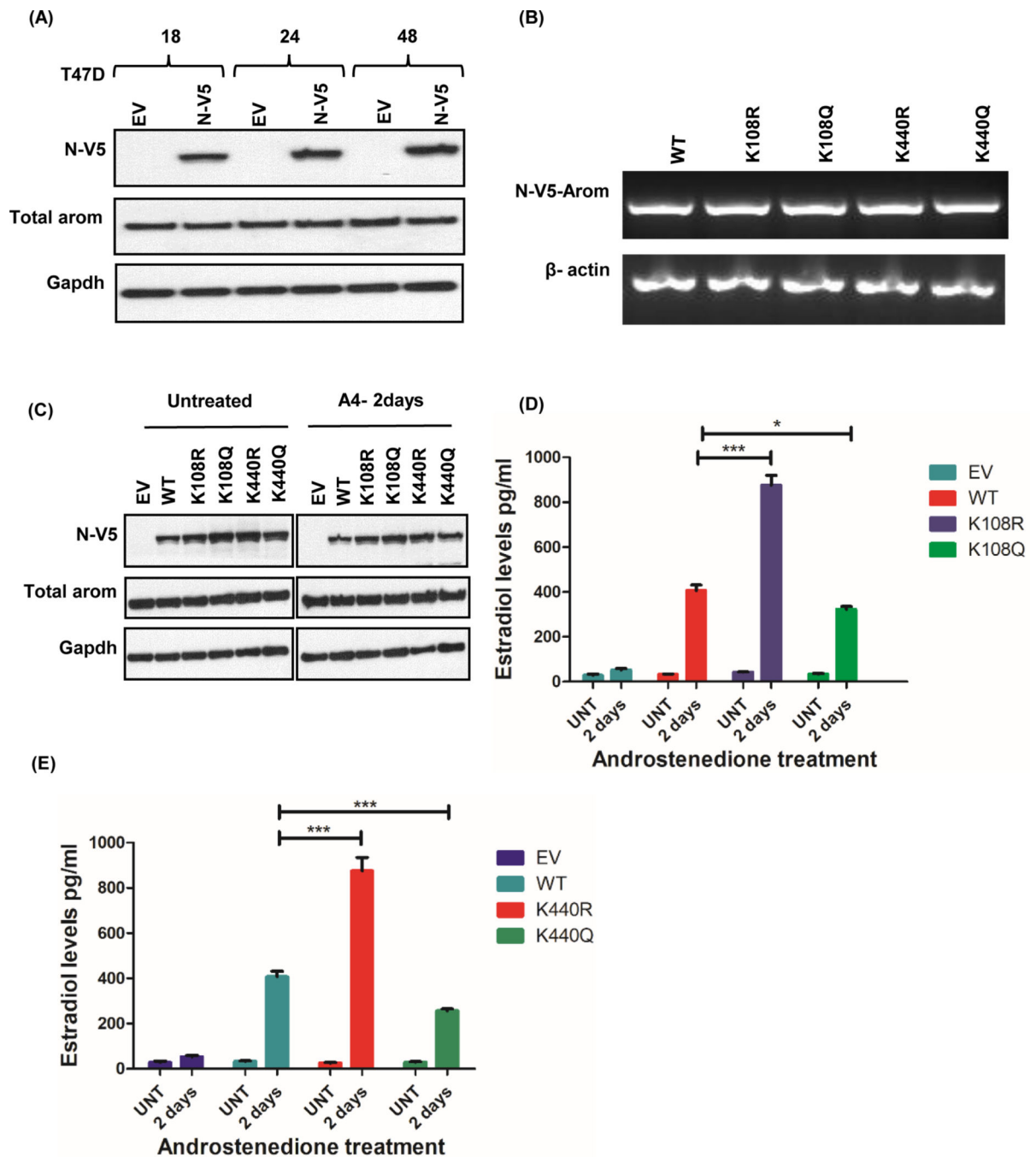
Figure 4: Aromatase constructs expressed in T47D cells alter aromatase activity.
A, Time course of N-V5-tagged aromatase-WT construct expression in T47D cells. **B,**
Transcript levels of V5-aromatase WT and mutant constructs and loading control beta actin
in T47D cells after 24hrs. **C,** Expression of N-terminally tagged V5-aromatase constructs,
endogenous aromatase (Total aromatase) and endogenous control Gapdh in T47D cells
untreated or treated with androstenedione for 2 days (A4–2days). **D,** Estradiol levels of V5-
aromatase WT and K108R/K108Q transfected cells treated with/without 10nM
androstenedione for 2 days (A4–2days). **E,** Estradiol levels of V5-aromatase WT and

K440R/K440Q transfected cells with/without 10nM androstenedione after 2 days (A4–2 days). Data is representative of three independent experiments carried out in triplicates with mean $\pm$ SEM *** $p<0.0001$, * $p<0.05$.
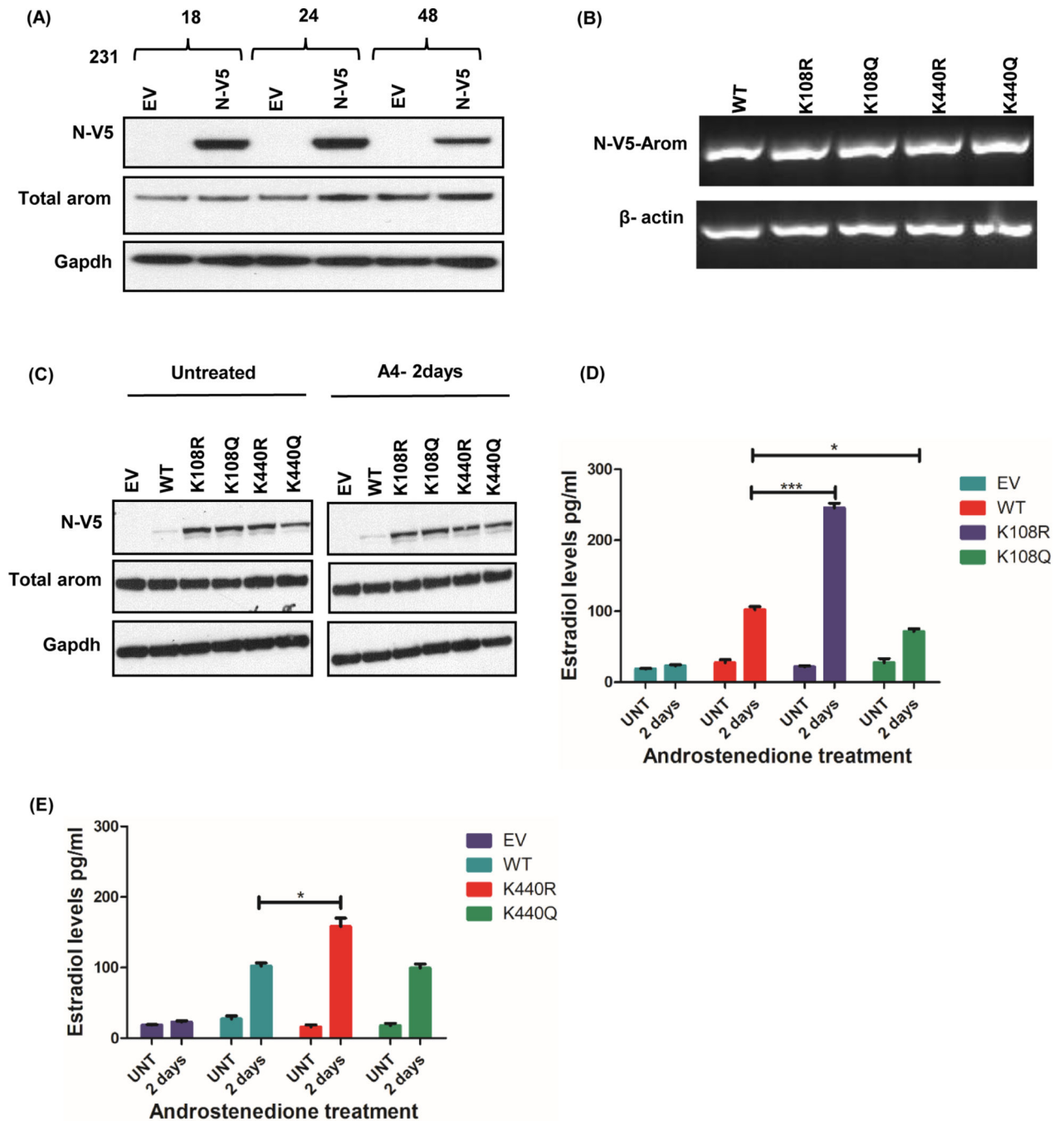
Figure 5: Aromatase constructs expressed in MDA-MB-231 cells alter aromatase activity.
A, Time course of N-V5-tagged aromatase-WT construct expression in 231 cells. **B,**
Transcript levels of V5-aromatase WT and mutant constructs and loading control beta actin
in 231 cells after 24hrs. **C,** Expression of N-terminally tagged V5-aromatase constructs,
endogenous aromatase (Total aromatase) and endogenous control Gapdh in 231 cells
untreated or treated with androstenedione for 2 days (A4–2days). **D,** Estradiol levels of V5-
aromatase WT and K108R/K108Q transfected cells treated with/without 10nM
androstenedione for 2 days (A4–2days). **E,** Estradiol levels of V5-aromatase WT and

K440R/K440Q transfected cells with/without 10nM androstenedione after 2 days (A4–2 days). Data is representative of three independent experiments carried out in triplicates with mean ± SEM *** $p<0.0001$, * $p<0.05$.
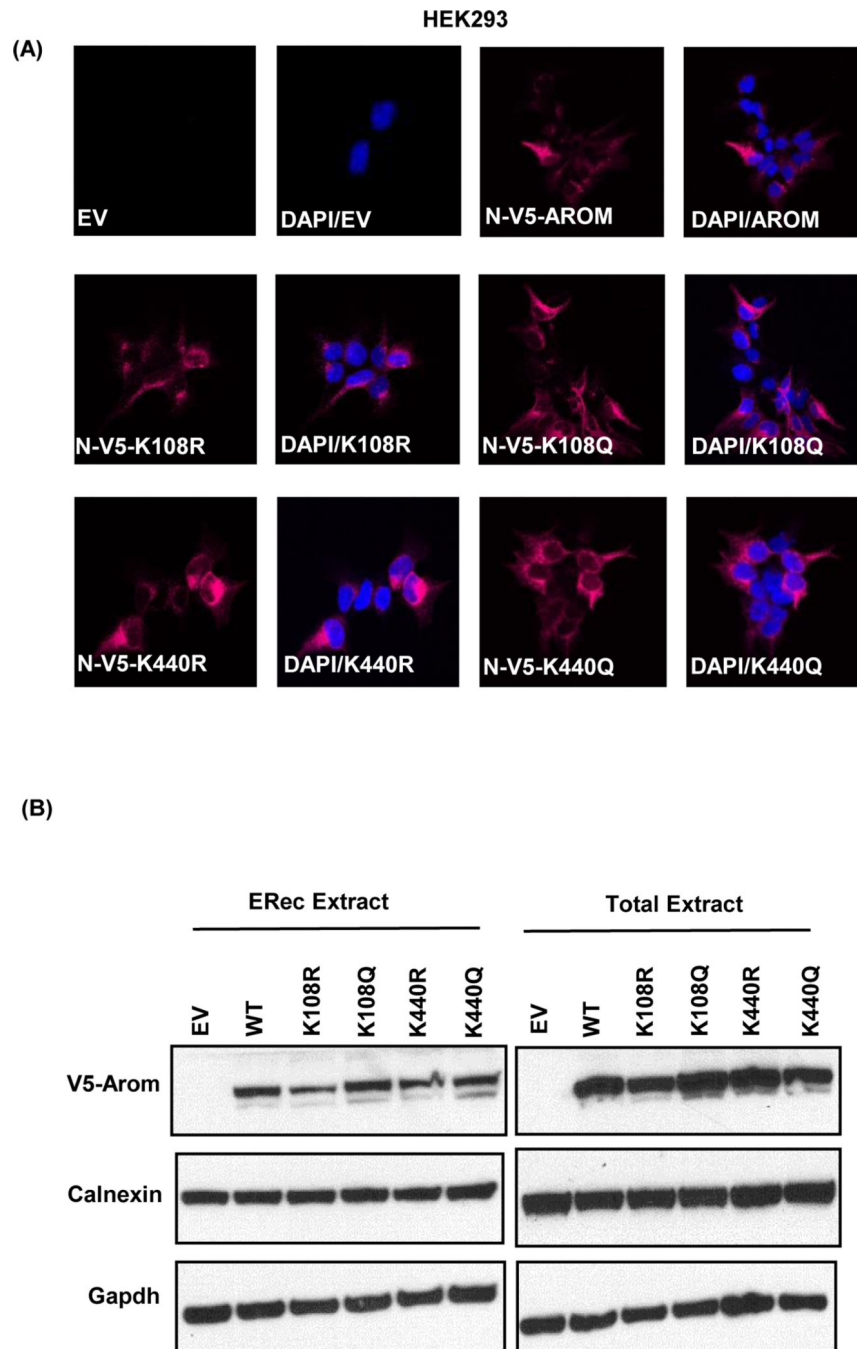
Figure 6: K108/K440 mutations do not change the subcellular localization of aromatase.
A, representative fluorescence images of N-V5-aromatase (magenta) in stably transfected HEK293 cells with empty vector (EV), N-V5-aromatase (N-V5-AROM), K108R mutant (N-V5-K108R), K108Q mutant (N-V5-K108Q), K440R mutant (N-V5-K440R) and K440Q mutant (N-V5-K440Q) proteins are shown. Merge of nuclear staining with DAPI (blue) and N-V5-aromatase (magenta) proteins is shown as DAPI/AROM for each of the mutant. **B,** Endoplasmic reticulum fractions (ERec extract) and total cell extract of HEK293 cells stably

transfected with WT and mutant aromatase constructs showing V5-aromatase, calnexin and Gapdh endogenous control.

(A)

PTM-IP

MCF-7

Arom

IgG-Lc

(Lanes: IgG, Ubiquitin, IgG, Sumo, Pan-methyl, Di-methyl, WCE)

(B)

Ubiquitin-IP

Ub-V5

IgG-Lc

Total V5

Gapdh

(Lanes: IgG, WT, K108R, K108Q, K440R, K440Q)

(C)

Sumo-1-IP

Sumo-V5

IgG-Lc

Total V5

Gapdh

(Lanes: IgG, WT, K108R, K108Q, K440R, K440Q)

(D)

Pan-methyl-IP

Kme-V5

IgG-Lc

Total V5

Gapdh

(Lanes: IgG, WT, K108R, K108Q, K440R, K440Q)
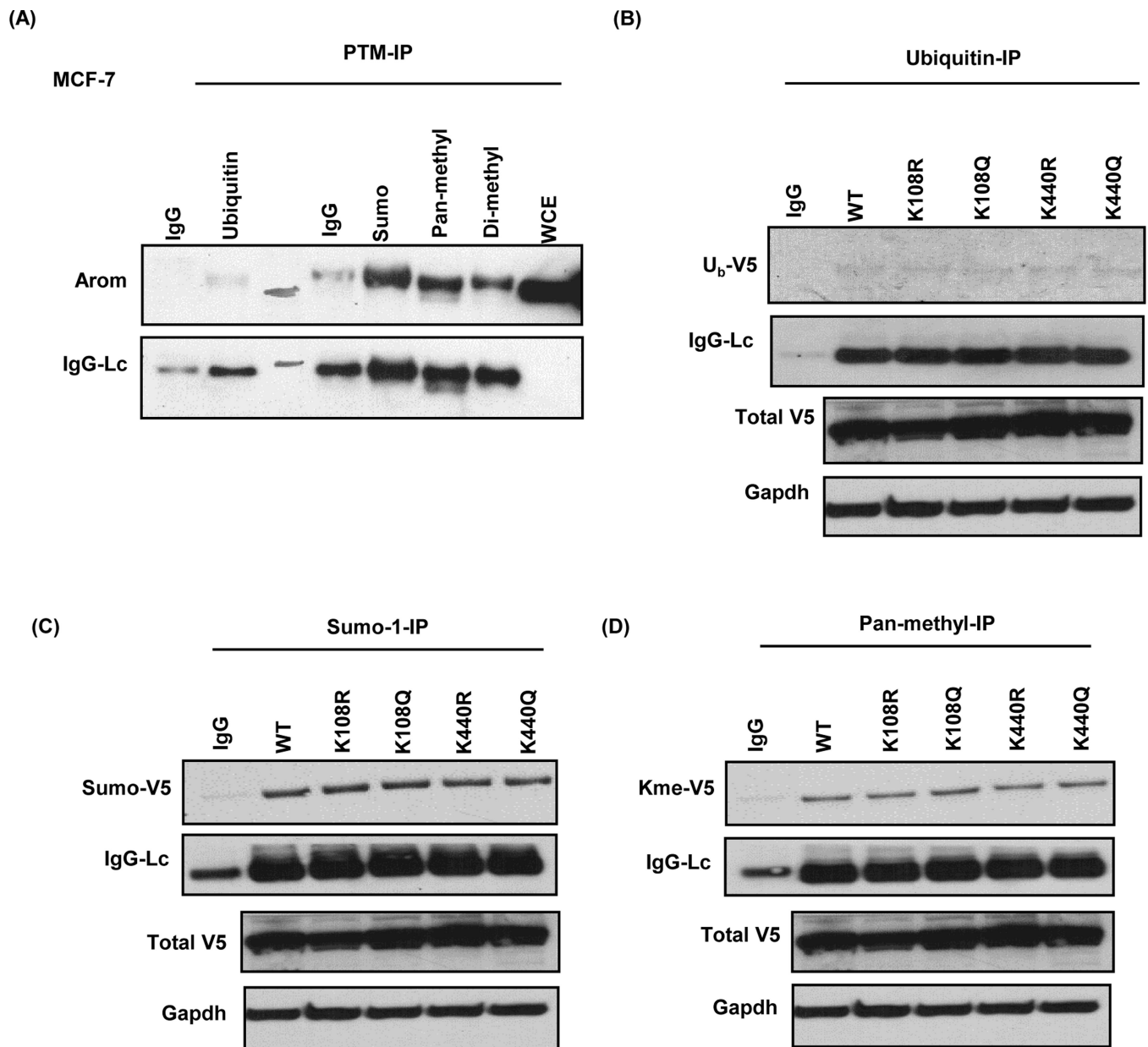
Figure 7: Endogenous and exogenous V5-aromatase are modified by PTMs.
A, Basal aromatase (arom) protein ubiquitination, sumoylation and methylation pattern and light chain (IgG-Lc) in MCF-7 cells. **B,** Ubiquitinated V5-aromatase (Ub-V5), light chain (IgG-Lc), total V5-aromatase (V5-arom) and Gapdh endogenous control (gapdh) in stably transfected MCF-7 cells. **C,** Sumoylated V5-aromatase (Sumo-V5), light chain (IgG-Lc), total V5-aromatase (V5-arom) and Gapdh in stably transfected MCF-7 cells. **D,** Pan-methylated V5-aromatase (Kme-V5), light chain (IgG-Lc), total V5-aromatase (V5-arom) and Gapdh in stably transfected MCF-7 cells.

Table 1:

Structural location of novel acetylated lysine residues and predicted functional role of domains in aromatase protein

Lysine	20% O$_2$		2.5% O$_2$		Structural location	Functional predictions
	Basal	Induced	Basal	Induced		
K108	+	+		+	Helix B	Substrate binding
K169	+	+	+	+	Helix D	Structural domain
K242	+	+	+	+	Helix G	Conformation of the active site
K262	+				Helix G	Structural domain
K334	+	+	+	+	Helix J	Substrate binding
K352	+		+		Loop region	Substrate binding
K354	+	+			Helix K	Substrate binding
K376		+		+	Major β-sheet β3	Substrate binding
K390		+			Loop region	Substrate binding
K440				+	Helix L	Heme binding
K448		+			Helix L	Heme binding

Table 2:

K108 and K440 residues are subject to other PTMs basally and when substituted with arginine residues

Residue	PTM Modification	ModPred Score	Confidence
K108	Ubiquitination	0.54	low
	Acetylation	0.53	low
K108R	ADP-ribosylation	0.53	low
K108Q	Not modified		
K440	Acetylated	0.91	High
	Ubiquitinated	0.61	low
K440R	Methylation	0.79	Medium
K440Q	Not modified		